

Near threshold radiative 3π production in e^+e^- annihilation

A.Ahmedov^a, G.V.Fedotovich^b, E.A.Kuraev^c, Z.K.Silagadze^b

^aLaboratory of Particle Physics, JINR, 141980, Dubna, 141980 Russia

^bBudker Institute of Nuclear Physics, 630 090, Novosibirsk, Russia

^cLaboratory of Theoretical Physics, JINR, 141980, Dubna, Russia

Abstract

We consider the $\pi^+\pi^-\pi_0\gamma$ final state in electron-positron annihilation at cms energies not far from the threshold. Both initial and final state radiations of the hard photon are considered, but without interference between them. The amplitude for the final state radiation is obtained by using the effective Wess-Zumino-Witten Lagrangian for pion-photon interactions valid for low energies. In real experiments energies are never so small that ρ and ω mesons would have a negligible effect. So a phenomenological Breit-Wigner factor is introduced in the final state radiation amplitude to account for the vector mesons influence. Using radiative 3π production amplitudes, a Monte Carlo event generator is developed which could be useful in experimental studies.

1 Introduction

The new Brookhaven experimental result for the anomalous magnetic moment of the muon [1] aroused considerable interest in the physics community, because it was interpreted as indicating a new physics beyond the Standard Model [2]. However, such claims, too premature in our opinion, assume that the theoretical prediction for the muon anomaly is well understood at the level of necessary precision. Hadronic uncertainties become of main concern [3]. Fortunately the leading hadronic contribution is related to the hadronic corrections to the photon vacuum polarization function, which can be accurately calculated provided that the precise experimental data on the low-energy hadronic cross sections in the e^+e^- annihilation are at our disposal.

In the last few years high-statistics experimental data were collected in the ρ - ω region in Novosibirsk experiments at the VEPP-2M collider [4]. In this region the hadronic cross sections are dominated by the $e^+e^- \rightarrow 2\pi$ and $e^+e^- \rightarrow 3\pi$ channels. The former is of uppermost importance for reduction of errors in the evaluation of the hadronic vacuum polarization contribution to the muon $g-2$. Considerable progress was reported for this channel by the CMD-2 collaboration [5]. The $e^+e^- \rightarrow 3\pi$ channel, which gives a less important but still significant contribution to the hadronic error, was also investigated in the same experiment in the ω -meson region [6]. Such high precision experiments require accurate knowledge of various backgrounds. Among them the $e^+e^- \rightarrow 3\pi\gamma$ channel provides an important background needed to be well understood. This experimental necessity motivated our investigation of the three pion radiative production presented here. Besides, being of interest as an important background source, this process could be of interest by itself, because a detailed experimental study of the final state radiation will allow one to get important information about pion-photon dynamics at low energies. However, such an experimental investigation will require much more statistics than available in VEPP-2M experiments and maybe would be feasible only at ϕ -factories where the low energy region can be reached by radiative return technique as was recently been demonstrated in the KLOE experiment [7].

2 Initial state radiation

Let J_μ be the matrix element of the electromagnetic current between the vacuum and the $\pi^+\pi^-\pi^0$ final state. Then the initial state radiation (ISR) contribution to the $e^+e^- \rightarrow \pi^+\pi^-\pi^0\gamma$ process cross section is given at $O(\alpha^3)$ by the standard expression [8]

$$d\sigma_{ISR}(e^+e^- \rightarrow 3\pi\gamma) = \frac{e^6}{4(2\pi)^8(Q^2)^2} \left\{ \frac{Q^2}{4E^2} J \cdot J^* \left(\frac{p_+}{k \cdot p_+} - \frac{p_-}{k \cdot p_-} \right)^2 - \right. \\ - \frac{Q^2}{2E^2} \frac{p_+ \cdot J \ p_+ \cdot J^* + p_- \cdot J \ p_- \cdot J^*}{k \cdot p_+ k \cdot p_-} - \frac{J \cdot J^*}{2E^2} \left(\frac{k \cdot p_+}{k \cdot p_-} + \frac{k \cdot p_-}{k \cdot p_+} \right) + \ (1) \\ \left. + \frac{m_e^2}{E^2} \left(\frac{p_+ \cdot J}{k \cdot p_-} - \frac{p_- \cdot J}{k \cdot p_+} \right) \left(\frac{p_+ \cdot J^*}{k \cdot p_-} - \frac{p_- \cdot J^*}{k \cdot p_+} \right) \right\} d\Phi \equiv \frac{e^6}{4(2\pi)^8} |A_{ISR}|^2 d\Phi,$$

where $d\Phi$ stands for the Lorentz invariant phase space

$$d\Phi = \frac{d\vec{k}}{2\omega} \frac{d\vec{q}_+}{2E_+} \frac{d\vec{q}_-}{2E_-} \frac{d\vec{q}_0}{2E_0} \delta(p_+ + p_- - k - q_+ - q_- - q_0)$$

and $Q^2 = (q_+ + q_- + q_0)^2 = 4E(E - \omega)$ is the photon virtuality, E being the beam energy and ω – the energy of the γ quantum. Particle 4-momenta assignment can be read from the corresponding diagrams presented in Fig.1.

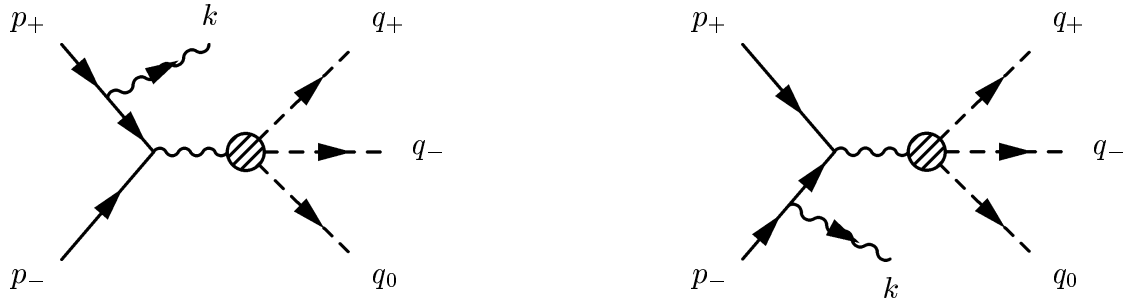


Figure 1: Initial state radiation diagrams and particle 4-momenta assignment.

The current matrix element J_μ has a general form

$$J_\mu = \epsilon_{\mu\nu\sigma\tau} q_+^\nu q_-^\sigma q_0^\tau F_{3\pi}(q_+, q_-, q_0). \quad (2)$$

For the $F_{3\pi}$ form-factor, which depends only on invariants constructed from the pions 4-momenta, we will take the expression from [9]

$$F_{3\pi} = \frac{\sqrt{3}}{(2\pi)^2 f_\pi^3} [\sin \theta \cos \eta \ R_\omega(Q^2) - \cos \theta \sin \eta \ R_\phi(Q^2)] (1 - 3\alpha_K - \alpha_K H). \quad (3)$$

Here $\alpha_K \approx 0.5$, $f_\pi \approx 93$ MeV is the pion decay constant, $\eta = \theta - \arcsin \frac{1}{\sqrt{3}} \approx 3.4^\circ$ characterizes the departure of the ω - ϕ mixing from the ideal one, and

$$H = R_\rho(Q_0^2) + R_\rho(Q_+^2) + R_\rho(Q_-^2),$$

where

$$Q_0^2 = (q_+ + q_-)^2, \quad Q_+^2 = (q_0 + q_+)^2, \quad Q_-^2 = (q_0 + q_-)^2.$$

The dimensionless Breit-Wigner factors have the form

$$R_V(Q^2) = \left[\frac{Q^2}{M_V^2} - 1 + i \frac{\Gamma_V}{M_V} \right]^{-1}, \quad R_\rho(Q^2) = \left[\frac{Q^2}{M_\rho^2} - 1 + i \frac{\sqrt{Q^2} \Gamma_\rho(Q^2)}{M_\rho^2} \right]^{-1},$$

where $V = \omega, \phi$ and for the ρ meson the energy dependent width is used

$$\Gamma_\rho(Q^2) = \Gamma_\rho \frac{M_\rho^2}{Q^2} \left(\frac{Q^2 - 4m\pi^2}{M_\rho^2 - 4m\pi^2} \right)^{3/2}.$$

The last term in (1) is completely irrelevant for VEPP-2M energies if the hard photon is emitted at a large angle. So we will neglect it in the following.

3 Final state radiation

To describe final state radiation (FSR), we use the effective low-energy Wess-Zumino-Witten Lagrangian [10]. The relevant piece of this Lagrangian is reproduced below

$$\begin{aligned} \mathcal{L} = & \frac{f_\pi^2}{4} Sp \left[D_\mu U (D_\mu U)^+ + \chi U^+ + U \chi^+ \right] - \\ & - \frac{e}{16\pi^2} \epsilon^{\mu\nu\alpha\beta} A_\mu Sp \left[Q \left\{ (\partial_\nu U) (\partial_\alpha U^+) (\partial_\beta U) U^+ - (\partial_\nu U^+) (\partial_\alpha U) (\partial_\beta U^+) U \right\} \right] - \\ & - \frac{ie^2}{8\pi^2} \epsilon^{\mu\nu\alpha\beta} (\partial_\mu A_\nu) A_\alpha Sp \left[Q^2 (\partial_\beta U) U^+ + Q^2 U^+ (\partial_\beta U) + \frac{1}{2} Q U Q U^+ (\partial_\beta U) U^+ - \right. \\ & \left. - \frac{1}{2} Q U^+ Q U (\partial_\beta U^+) U \right]. \end{aligned} \quad (4)$$

Here $U = \exp \left(i \frac{\sqrt{2}P}{f_\pi} \right)$, $D_\mu U = \partial_\mu U + ieA_\mu [Q, U]$, $Q = \text{diag} \left(\frac{2}{3}, -\frac{1}{3}, -\frac{1}{3} \right)$ is the quark charge matrix, and the terms with $\chi = B \text{diag} (m_u, m_d, m_s)$ introduce explicit chiral symmetry breaking due to nonzero quark masses.

The constant B has dimension of mass and is determined through the equation $Bm_q = m_\pi^2$, $m_q = m_u \approx m_d$. The pseudoscalar meson matrix P has its standard form

$$P = \begin{pmatrix} \frac{1}{\sqrt{2}}\pi^0 + \frac{1}{\sqrt{6}}\eta & \pi^+ & K^+ \\ \pi^- & -\frac{1}{\sqrt{2}}\pi^0 + \frac{1}{\sqrt{6}}\eta & K^0 \\ K^- & \bar{K}^0 & -\frac{2}{\sqrt{6}}\eta \end{pmatrix}.$$

It is straightforward to get from (4) the relevant interaction vertices shown in Fig.2.

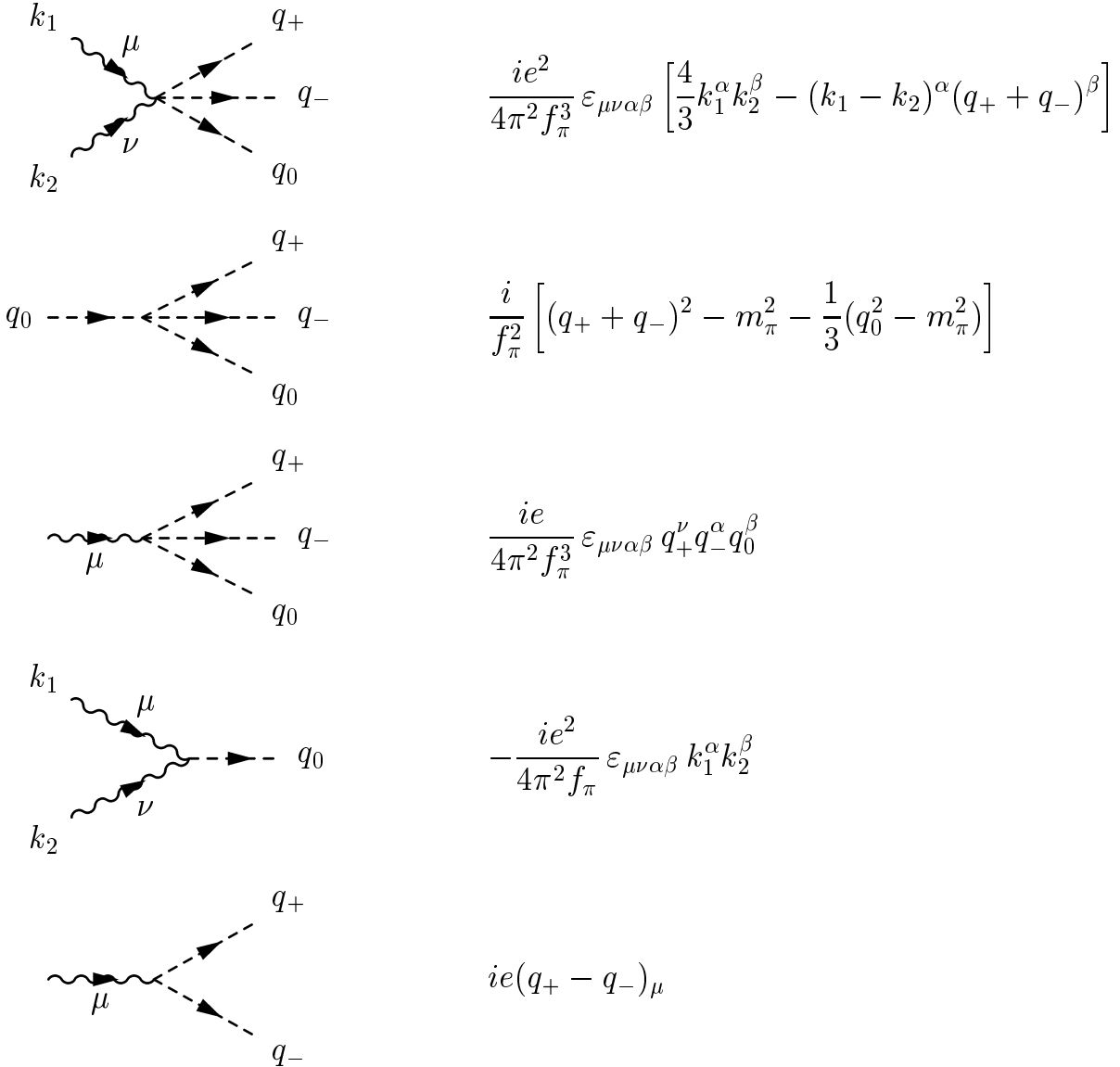


Figure 2: Interaction vertexes relevant for final state radiation.

Using these Feynman rules, one can calculate the $\gamma^* \rightarrow \pi^+ \pi^- \pi^0 \gamma$ amplitude originated from the diagrams shown in Fig.3.

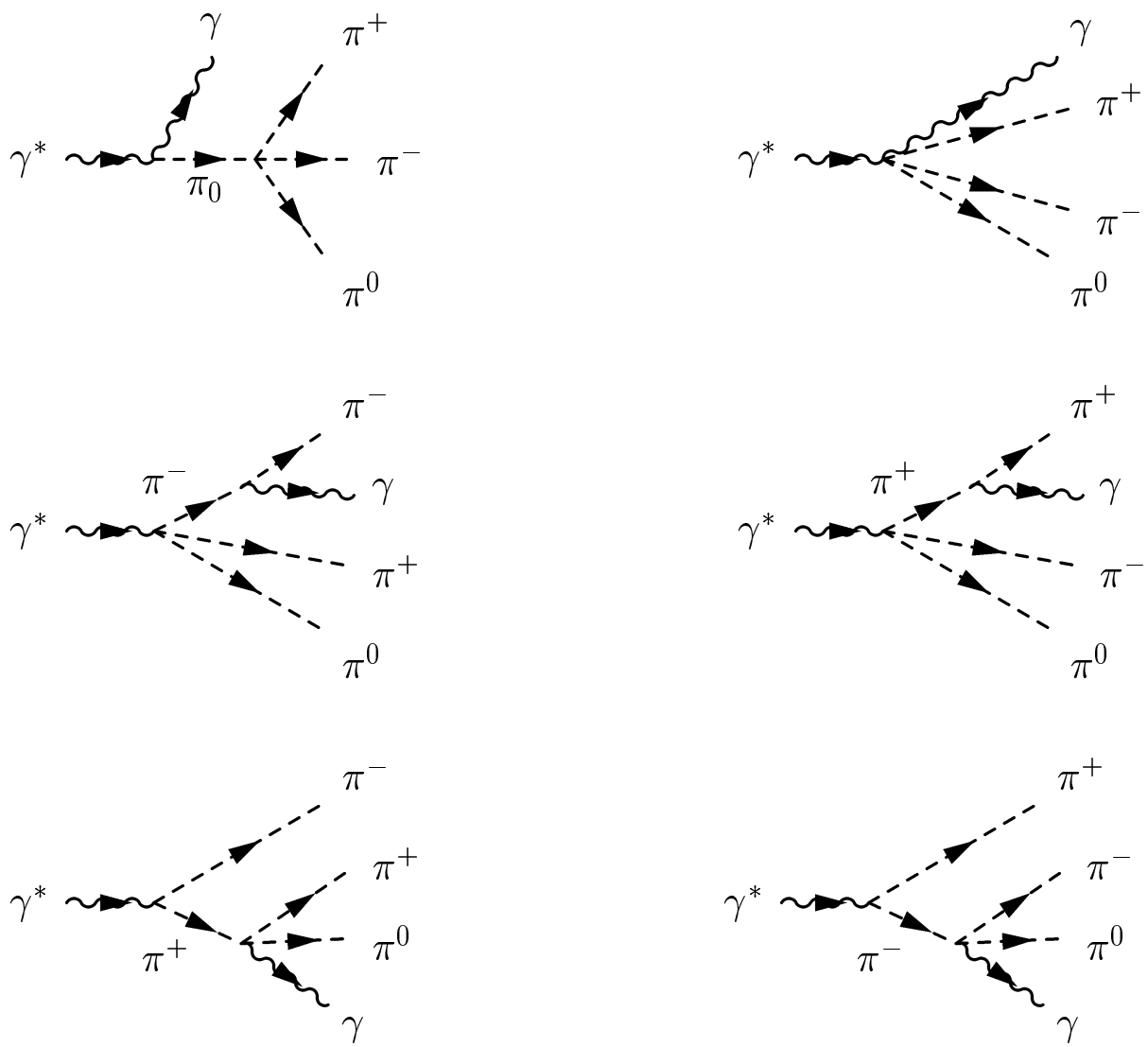


Figure 3: $\gamma^* \rightarrow \pi^+ \pi^- \pi^0 \gamma$ transition diagrams.

The result is

$$A_{\mu\nu}(\gamma_\mu^* \rightarrow 3\pi\gamma_\nu) = \frac{ie^2}{4\pi^2 f_\pi^3} T_{\mu\nu}, \quad (5)$$

where ($Q = q_+ + q_- + q_0 + k$ is the virtual photon 4-momentum)

$$\begin{aligned} T_{\mu\nu} = & \epsilon_{\mu\nu\alpha\beta} Q^\alpha k^\beta \left(1 - \frac{(q_+ + q_-)^2 - m_\pi^2}{(Q - k)^2 - m_\pi^2} \right) + \epsilon_{\mu\nu\alpha\beta} (Q + k)^\alpha q_0^\beta + \\ & + \epsilon_{\mu\lambda\alpha\beta} Q^\alpha q_0^\beta \left(\frac{(2q_- + k)_\nu q_+^\lambda}{2q_- \cdot k} + \frac{(2q_+ + k)_\nu q_-^\lambda}{2q_+ \cdot k} \right) - \\ & - \epsilon_{\nu\lambda\alpha\beta} k^\alpha q_0^\beta \left(\frac{(2q_- - Q)_\mu q_+^\lambda}{Q^2 - 2q_- \cdot Q} + \frac{(2q_+ - Q)_\mu q_-^\lambda}{Q^2 - 2q_+ \cdot Q} \right). \end{aligned} \quad (6)$$

The tensor $T_{\mu\nu}$ is gauge invariant

$$Q^\mu T_{\mu\nu} = k^\nu T_{\mu\nu} = 0.$$

Note that our result for $A_{\mu\nu}(\gamma_\mu^* \rightarrow 3\pi\gamma_\nu)$ is in agreement with the known result [11, 12] for the $\gamma^* \gamma^* \rightarrow 3\pi$ amplitude (these two amplitudes are connected by crossing symmetry, of course).

If $J_\mu^{(\gamma)}$ is the amplitude of the transition $\gamma_\mu^* \rightarrow \pi^+ \pi^- \pi^0 \gamma$, then the final state radiation (FSR) contribution to the $e^+ e^- \rightarrow \gamma^* \rightarrow \pi^+ \pi^- \pi^0 \gamma$ process cross section is given by [8]

$$\begin{aligned} d\sigma_{FSR} = & \frac{e^2}{(2\pi)^8 64E^4} \sum_\epsilon \left\{ \frac{Re(p_+ \cdot J^{(\gamma)} p_- \cdot J^{(\gamma)*})}{E^2} - J^{(\gamma)} \cdot J^{(\gamma)*} \right\} d\Phi \approx \\ & \approx \frac{e^2}{(2\pi)^8 64E^4} \sum_\epsilon \left[|J_1^{(\gamma)}|^2 + |J_2^{(\gamma)}|^2 \right] d\Phi, \end{aligned}$$

where the sum is over the photon polarization ϵ and the z axis was assumed to be along \vec{p}_- , but $J_\mu^{(\gamma)} = \epsilon^\nu A_{\mu\nu}(\gamma^* \rightarrow 3\pi\gamma)$. So we can perform the polarization sum by using $\sum_\epsilon \epsilon_\mu \epsilon_\nu^* = -g_{\mu\nu}$. By introducing gauge invariant real 4-vectors t_1 and t_2 via $t_{1\mu} = T_{1\mu}$, $t_{2\mu} = T_{2\mu}$, the result can be casted in the form (note that the norm of the gauge invariant 4-vector is always negative)

$$d\sigma_{FSR}(e^+ e^- \rightarrow 3\pi\gamma) = \frac{e^6}{(2\pi)^8 64E^4} \frac{1}{(2\pi)^4 f_\pi^6} [-t_1 \cdot t_1 - t_2 \cdot t_2] d\Phi. \quad (7)$$

However, for the photon virtualities of real experimental interest vector meson effects can no longer be neglected. So we replace (7) by

$$d\sigma_{FSR}(e^+ e^- \rightarrow 3\pi\gamma) = \frac{e^6}{(2\pi)^8 64E^4} \frac{1}{(2\pi)^4 f_\pi^6} [-t_1 \cdot t_1 - t_2 \cdot t_2] K_{BW} d\Phi \equiv$$

$$\equiv \frac{e^6}{4(2\pi)^8} |A_{FSR}|^2 d\Phi, \quad (8)$$

where we have introduced the phenomenological Breit-Wigner factor

$$K_{BW} = 3 |\sin \theta \cos \eta R_\omega(4E^2) - \cos \theta \sin \eta R_\phi(4E^2)|^2.$$

This factor is similar to one presented in ISR (see (3)) and tends to unity as $E \rightarrow 0$. It gives about an order of magnitude increase in σ_{FSR} for energies $2E = 0.65 \div 0.7$ GeV.

4 Monte-Carlo event generator

Although what follows can be considered as a textbook material [13], we will nevertheless give a somewhat detailed description of the Monte Carlo algorithm for the sake of convenience.

The important first step is the following transformation of the Lorentz invariant phase space. Let $R_n(p^2; m_1^2, \dots, m_n^2)$ be n -particle phase space

$$R_n(p^2; m_1^2, \dots, m_n^2) = \int \prod_{i=1}^n \frac{d\vec{q}_i}{2E_i} \delta(p - \sum_{i=1}^n q_i).$$

Inserting the identity

$$1 = \int dk_1 d\mu_1^2 \delta(p - q_1 - k_1) \delta(k_1^2 - \mu_1^2)$$

we get

$$\begin{aligned} R_4(p^2; m_1^2, m_2^2, m_3^2, m_4^2) &= \int \frac{d\vec{q}_1}{2E_1} R_3((p - q_1)^2; m_2^2, m_3^2, m_4^2) = \\ &= \int \frac{d\vec{q}_1}{2E_1} dk_1 d\mu_1^2 R_3(k_1^2; m_2^2, m_3^2, m_4^2) \delta(p - q_1 - k_1) \delta(k_1^2 - \mu_1^2). \end{aligned}$$

However, (note that $(p - q_1)_0 = E_2 + E_3 + E_4 > 0$)

$$\int \frac{d\vec{q}_1}{2E_1} dk_1 \delta(k_1^2 - \mu_1^2) \delta(p - q_1 - k_1) = \int \frac{d\vec{q}_1}{2E_1} \frac{d\vec{k}_1}{2k_{10}} \delta(p - q_1 - k_1) = R_2(p^2; m_1^2, \mu_1^2).$$

Therefore,

$$R_4(p^2; m_1^2, m_2^2, m_3^2, m_4^2) = \int d\mu_1^2 R_3(\mu_1^2; m_2^2, m_3^2, m_4^2) R_2(p^2; m_1^2, \mu_1^2). \quad (9)$$

But [13]

$$R_2(p^2; m_1^2, \mu_1^2) = \int \frac{\lambda^{1/2}(p^2; m_1^2, \mu_1^2)}{8p^2} d\Omega_1^*$$

where λ stands for the triangle function and Ω_1^* describes the orientation of the \vec{q}_1 vector in the p -particle rest frame.

It is more convenient to integrate over q -particle energy E^* instead of mass μ , the two being interconnected by the relation $\mu^2 = p^2 + q^2 - 2\sqrt{p^2}E^*$ in the p -particle rest frame.

Using the relation [13]

$$\frac{\lambda^{1/2}(p^2; m^2, \mu^2)}{2\sqrt{p^2}} = \mu\sqrt{\bar{\gamma}^2 - 1},$$

where $\bar{\gamma}$ is the γ -factor of the “particle” (subsystem) with the invariant mass μ , after repeatedly using (9) we get

$$R_4 = \int \frac{1}{2}\sqrt{\bar{\gamma}_1^2 - 1} dE_1^* d\Omega_1^* \frac{1}{2}\mu_1\sqrt{\bar{\gamma}_2^2 - 1} dE_2^* d\Omega_2^* \frac{1}{2}|\vec{p}_3^*| d\Omega_3^*,$$

where \vec{p}_3^* momentum is in the rest frame of the (3,4) subsystem, and E_2^* , Ω_2^* , $\bar{\gamma}_2$ are in the rest frame of the (2,3,4) subsystem.

Now it is straightforward to rewrite the differential cross-section in the following form:

$$d\sigma(e^+e^- \rightarrow 3\pi\gamma) = \frac{\alpha^3}{2\pi^2} |A|^2 f d\Phi^*, \quad (10)$$

where $|A|^2 = |A_{ISR}|^2 + |A_{FSR}|^2$ (we do not take into account the interference between the initial and final state radiations. This interference integrates to zero if we do not distinguish between negative and positive π -mesons),

$$f = \mu_1(\omega_{max} - \omega_{min})(E_{0\ max}^* - E_{0\ min}^*)\sqrt{(E_{-}^* - m_\pi^2)(\bar{\gamma}_1^2 - 1)(\bar{\gamma}_2^2 - 1)}, \quad (11)$$

and

$$d\Phi^* = \frac{d\omega}{(\omega_{max} - \omega_{min})} \frac{d\varphi}{2\pi} \frac{d\cos\theta}{2} \frac{dE_0^*}{(E_{0\ max}^* - E_{0\ min}^*)} \frac{d\varphi_0^*}{2\pi} \frac{d\cos\theta_0^*}{2} \frac{d\varphi_-^*}{2\pi} \frac{d\cos\theta_-^*}{2}. \quad (12)$$

The upper and lower limits for energies are

$$\omega_{max} = \frac{s - 9m_\pi^2}{2\sqrt{s}}, \quad E_{0\ max}^* = \frac{\mu_1^2 - 3m_\pi^2}{2\mu_1}, \quad E_{0\ min}^* = m_\pi.$$

The minimal photon energy ω_{min} is an external experimental cut. At last, $|A_{ISR}|^2$ and $|A_{FSR}|^2$ can be read from the corresponding expressions (1) and (8), respectively.

According to (10), we can generate $e^+e^- \rightarrow \pi^+\pi^-\pi^0\gamma$ events in the cms frame by the following algorithm.

- generate the photon energy ω as a random number uniformly distributed from ω_{min} to ω_{max} . Calculate for the $S_1 = (\pi^+ \pi^- \pi^0)$ subsystem the energy $\bar{E}_1 = 2E - \omega$, invariant mass $\bar{\mu}_1 = \sqrt{4E(E - \omega)}$ and the Lorentz factor $\bar{\gamma}_1 = \bar{E}_1/\bar{\mu}_1$.

• generate a random number $\bar{\varphi}_1$ uniformly distributed in the interval $[0, 2\pi]$ and take it as an azimuthal angle of the S_1 subsystem velocity vector in the cms frame. Generate another uniform random number in the interval $[-\cos \theta_{min}, \cos \theta_{min}]$ and take it as a $\cos \bar{\theta}_1$, $\bar{\theta}_1$ being the polar angle of the S_1 subsystem velocity vector in the cms frame. This defines the unit vector $\vec{n}_1 = (\sin \bar{\theta}_1 \cos \bar{\varphi}_1, \sin \bar{\theta}_1 \sin \bar{\varphi}_1, \cos \bar{\theta}_1)$ along the S_1 subsystem velocity; θ_{min} is the minimal photon radiation angle – an external experimental cut.

- construct the photon momentum in the cms frame $\vec{k} = -\omega \vec{n}_1$.
- generate the π^0 -meson energy E_0^* in the S_1 rest frame as a random number uniformly distributed from $E_{0\ min}^*$ to $E_{0\ max}^*$. Calculate for the $S_2 = (\pi^+, \pi^-)$ subsystem the energy $\bar{E}_2 = \bar{\mu}_1 - E_0^*$, invariant mass $\bar{\mu}_2 = \sqrt{\bar{\mu}_1^2 + m_\pi^2 - 2\bar{\mu}_1 E_0^*}$ and the Lorentz factor $\bar{\gamma}_2 = \bar{E}_2/\bar{\mu}_2$.

• generate a random number $\bar{\varphi}_2$ uniformly distributed in the interval $[0, 2\pi]$ and take it as an azimuthal angle of the S_2 subsystem velocity vector in the S_1 rest frame. Generate another uniform random number in the interval $[-1, 1]$ and take it as a $\cos \bar{\theta}_2$, $\bar{\theta}_2$ being the polar angle of the S_2 subsystem velocity vector in the S_1 rest frame. This defines the unit vector along the S_2 subsystem velocity in the S_1 rest frame $\vec{n}_2 = (\sin \bar{\theta}_2 \cos \bar{\varphi}_2, \sin \bar{\theta}_2 \sin \bar{\varphi}_2, \cos \bar{\theta}_2)$.

- construct $\vec{q}_0^* = -\sqrt{E_0^{*2} - m_\pi^2} \vec{n}_2$ – the π^0 -meson momentum in the S_1 rest frame.

• generate φ_-^* and $\cos \theta_-^*$ in the manner analogous to what was described above for $\bar{\varphi}_2$ and $\cos \bar{\theta}_2$ and construct the unit vector along the π^- meson velocity in the S_2 rest frame $\vec{n}_3 = (\sin \theta_-^* \cos \varphi_-^*, \sin \theta_-^* \sin \varphi_-^*, \cos \theta_-^*)$.

- construct the π^- -meson 4-momentum in the S_2 rest frame $E_-^* = \bar{\mu}_2/2$, $\vec{q}_-^* = \sqrt{E_-^{*2} - m_\pi^2} \vec{n}_3$.

- construct the π^+ -meson 4-momentum in the S_2 rest frame $E_+^* = \bar{\mu}_2/2$, $\vec{q}_+^* = -\vec{q}_-^*$.

• transform π^0 -meson 4-momentum from the S_1 rest frame back to the cms frame.

• transform π^- and π^+ mesons 4-momenta firstly from the S_2 rest frame to the S_1 rest frame and then back to the cms frame.

• for the generated 4-momenta of the final state particles, calculate $z = |A|^2 f$.

- generate a random number z_R uniformly distributed in the interval from 0 to z_{max} where z_{max} is some number majoring $|A|^2 f$ for all final state 4-momenta allowed by 4-momentum conservation.
- if $z \geq z_R$, accept the event that is the generated 4-momenta of the π^+ , π^- and π^0 mesons and the photon. Otherwise repeat the whole procedure.

5 Soft and collinear photon corrections

We assume that the photon in the $e^+e^- \rightarrow 3\pi\gamma$ reaction is hard enough $\omega > \omega_{min}$ and radiated at large angle $\theta > \theta_{min}$ so that it could be detected by experimental equipment (a detector). In any process with accelerated charged particles soft photons are emitted without being detected because a detector has finite energy resolution. Even moderately hard photons can escape detection in some circumstances. How important are such effects? Naively every photon emitted brings extra factor e in the amplitude and so a small correction is expected. But this argument (as well as the perturbation theory) breaks down for soft photons. When an electron (positron) emits a soft enough photon, it nearly remains on the mass shell, thus bringing a very large propagator in the amplitude. Formal application of the perturbation theory gives an infinite answer to the correction due to soft photon emission because of this pole singularity. It is well known [14] how to deal with this infrared divergence. In real experiments very low energy photons never have enough time and space to be formed, because of a finite size of the laboratory. So we have a natural low energy cut-off. A remarkable fact, however, is that the observable cross sections do not depend on the actual form of the cut-off because singularities due to real and virtual soft photons cancel each other [15]. The net effect is that the soft photon corrections, summed to all orders of perturbation theory, factor out as some calculable, so called Yennie-Frautschi-Suura exponent [14].

Collinear radiation of (not necessarily soft) photons by highly relativistic initial electrons (positrons) is another source of big corrections which should also be treated non-perturbatively. Unlike soft photons, however, the matrix element for a radiation of an arbitrary number of collinear photons is unknown. Nevertheless, there is a nice method (the so called Structure Functions method) [16] which enables one to sum leading collinear (and soft) logarithms. The corrected cross-section, when radiation of unnoticed photons with total energy less than $\Delta E \ll E$ is allowed, looks like

[16]

$$\tilde{\sigma}(s) = \int_0^{\Delta E} \frac{d\omega}{\omega} \sigma(4E(E-\omega)) \beta \left(\frac{\omega}{E}\right)^\beta \left[1 + \frac{3}{4}\beta + \frac{\alpha}{\pi} \left(\frac{\pi^2}{3} - \frac{1}{2}\right)\right], \quad (13)$$

where $\beta = \frac{2\alpha}{\pi} \left(\ln \frac{s}{m_e^2} - 1\right)$ and we have omitted some higher order terms.

In our case the hard photon is well separated (because of $\omega > \omega_{min}$, $\theta > \theta_{min}$ cuts) from the soft and collinear regions of the phase space. So equation (13) is applicable and it indicates that the soft and collinear corrections to the cross-section of the process $e^+e^- \rightarrow 3\pi\gamma$ do not exceed 20% when $\Delta E \sim \omega_{min} = 30$ MeV, $\theta_{min} = 20^\circ$ and $E = 0.7$ GeV. Such corrections are irrelevant for the present VEPP-2M statistics but may become important in future high statistics experiments.

6 Numerical results and conclusions

In Fig.4, numerical results are shown for $\sigma(e^+e^- \rightarrow 3\pi\gamma)$ with $\omega_{min} = 30$ MeV, $\theta_{min} = 20^\circ$. As expected, the cross section is small, only few picobarns, for energies $0.65 \div 0.7$ GeV.

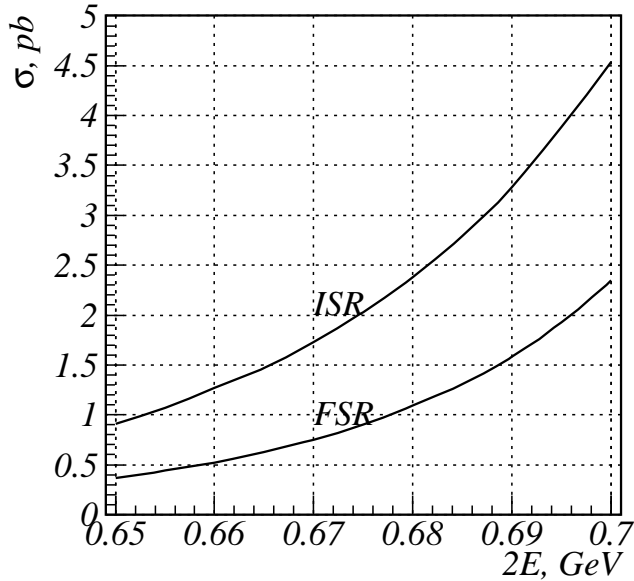


Figure 4: ISR and FSR contributions to the $e^+e^- \rightarrow 3\pi\gamma$ cross section.

This figure shows also that FSR contributes significantly at such low energies. So if future ϕ -factory experiments produce high enough statistics in this energy region, the study of FSR will become realistic. ISR and FSR

give different angular and energy distributions for the photon as illustrated by Fig.5 and Fig.6. This fact can be used for the FSR separation from a somewhat more intensive ISR.

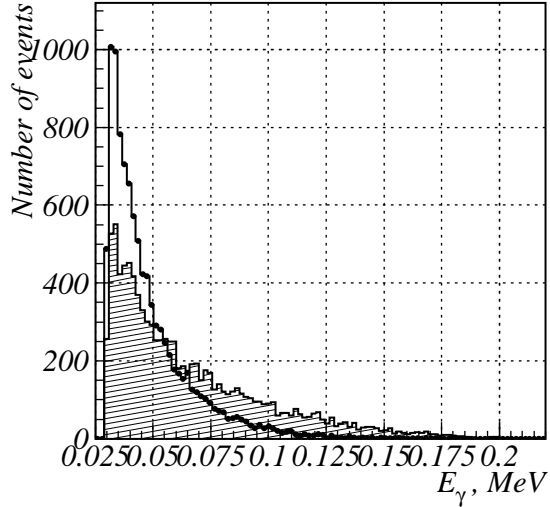


Figure 5: The photon energy distributions for ISR and FSR (hatched histogram).

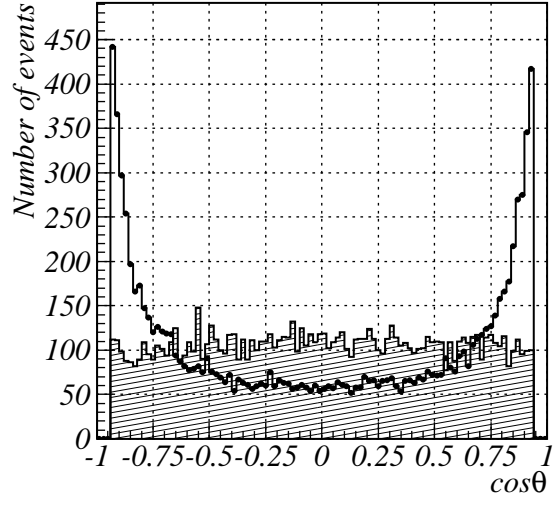


Figure 6: The photon angular distributions for ISR and FSR (hatched histogram).

Let us note, however, that the model considered here is not valid in the ϕ -meson region – very far from the threshold. At that the status of uncertainties in the ISR and FSR contributions are different. We believe that the ISR amplitude remains accurate enough even in the ϕ -meson region. This belief stems from the fact that all relevant vector meson effects are already included in the ISR amplitude (3). The situation with the FSR amplitude is different. Our phenomenological Breit-Wigner factor mimics only some part of the vector meson effects. To estimate the corresponding uncertainty in σ_{FSR} , let us try some other choices for K_{BW} which also have the correct low energy limit. If in the expression for the K_{BW} factor we make the change

$$R_\omega(4E^2) \rightarrow \frac{1}{2} [R_\omega(4E^2) + R_\rho(4E^2)],$$

σ_{FSR} will be lowered by $\sim 5\%$ for $2E = 0.65$ GeV, and by $\sim 25\%$ for $2E = 0.7$ GeV. In the FSR amplitude the ρ -meson contributes via a number of various diagrams. For example, the $\gamma^* \rightarrow \rho \rightarrow \rho^+ \rho^- \rightarrow \pi^+ \pi^0 \pi^- \gamma$ intermediate state, which has no counterpart in the ω meson contribution, gives the following piece of the $T_{\mu\nu}$ tensor

$$T_{\mu\nu}^{(3\rho)} = -\frac{\alpha_K}{2} R_\rho(4E^2) \left\{ A_1 - 2A_2 - 2A_3 \right\},$$

where

$$\begin{aligned}
A_1 &= \epsilon_{\nu\alpha\beta\lambda} (Q - 2q_0)^\alpha k^\beta \left[(q_+ + q_0 - q_- - k)_\mu q_-^\lambda Y_- + \right. \\
&\quad \left. + (q_- + q_0 - q_+ - k)_\mu q_+^\lambda Y_+ \right], \\
A_2 &= \epsilon_{\nu\alpha\beta\lambda} Q^\alpha k^\beta \left[(q_+ - q_0)_\mu q_-^\lambda Y_- + (q_- - q_0)_\mu q_+^\lambda Y_+ \right], \\
A_3 &= \epsilon_{\mu\nu\beta\lambda} k^\beta \left[Q \cdot (q_+ - q_0) q_-^\lambda Y_- + Q \cdot (q_- - q_0) q_+^\lambda Y_+ \right],
\end{aligned}$$

and

$$Y_\mp = \frac{M_\rho^2}{[(q_\mp + k)^2 - M_\rho^2][(q_\pm + q_0)^2 - M_\rho^2]}.$$

If we include this contribution, and besides ensure that the remaining part of the FSR amplitude (6) also takes

$$K_{BW} = |R_\rho(4E^2)|^2$$

in the role of the phenomenological Breit-Wigner factor, the FSR cross section will be lowered by $\sim 10\%$ for $2E = 0.65$ GeV, and by $\sim 35\%$ for $2E = 0.7$ GeV.

This uncertainty in the FSR magnitude is irrelevant for the present VEPP-2M statistics. For future high precision experiments a systematic inclusion of all relevant vector meson effects in the FSR amplitude is desired.

Acknowledgments

One of us (EAK) is grateful to Heisenberg-Landau Fund 2000-02 and to RFFI Grant 99-02-17730. We are grateful to G. Sandukovskaya for the help.

References

- [1] H. N. Brown *et al.* [Muon g-2 Collaboration], Phys. Rev. Lett. **86**, 2227 (2001).
- [2] For review see, for example
A. Czarnecki and W. J. Marciano, Phys. Rev. D **64**, 013014 (2001).
- [3] K. Melnikov, Int. J. Mod. Phys. A **16**, 4591 (2001);
J. F. De Troconiz and F. J. Yndurain, hep-ph/0106025;
M. Knecht and A. Nyffeler, hep-ph/0111058.

- [4] M. N. Achasov *et al.*, hep-ex/0010077.
 R. R. Akhmetshin *et al.* [CMD-2 Collaboration], Nucl. Phys. A **675**, 424C (2000).
- [5] R. R. Akhmetshin *et al.* [CMD-2 Collaboration], hep-ex/9904027.
- [6] R. R. Akhmetshin *et al.* [CMD-2 Collaboration], Phys. Lett. B **476**, 33 (2000).
- [7] A. Aloisio *et al.* [KLOE Collaboration], hep-ex/0107023.
- [8] G. Bonneau and F. Martin, Nucl. Phys. B **27**, 381 (1971).
- [9] E. A. Kuraev and Z. K. Silagadze, Phys. Atom. Nucl. **58**, 1589 (1995)
- [10] E. Witten, Nucl. Phys. B **223**, 422 (1983).
 J. Wess and B. Zumino, Phys. Lett. B **37**, 95 (1971).
- [11] J. W. Bos, Y. C. Lin and H. H. Shih, Phys. Lett. B **337**, 152 (1994).
- [12] P. Talavera, L. Ametller, J. Bijnens, A. Bramon and F. Cornet, Phys. Lett. B **376**, 186 (1996);
 L. Ametller, J. Kambor, M. Knecht and P. Talavera, Phys. Rev. D **60**, 094003 (1999).
- [13] E. Byckling and K. Kajantie, *Particle Kinematics*. Wiley, 1973.
- [14] D. R. Yennie, S. C. Frautschi and H. Suura, Annals Phys. **13**, 379 (1961).
- [15] F. Bloch and A. Nordsieck, Phys. Rev. **52**, 54 (1937).
 D. R. Yennie, in Lectures on strong and electromagnetic interactions, p. 166 (Brandies Summer Institute in Theoretical Physics, Waltman, Mass., 1963)
- [16] E. A. Kuraev and V. S. Fadin, Sov. J. Nucl. Phys. **41**, 466 (1985).
 For review see M. Skrzypek, Acta Phys. Polon. B **23**, 135 (1992).